TRAJECTORY TRACKING CONTROL FOR A DIFFERENTIAL DRIVE MOBILE ROBOT WITH LOAD OFFSETTING

Ling Zhao[1,*], Zixing Nie[1], Jinchao Li[1] and Hongjiu Yang[2]

[1]State Key Laboratory of Precision Measuring Technology and Instruments
[2]School of Electrical and Information Engineering
Tianjin University
No. 92, Weijin Road, Nankai District, Tianjin 300072, P. R. China
{ niezx; ljc981101; yanghongjiu }@tju.edu.cn
*Corresponding author: ling.zhao@tju.edu.cn

ABSTRACT. *In this paper, a double closed-loop tracking control strategy is proposed to achieve trajectory tracking for a differential drive mobile robot with load offsetting. A nonlinear extend state observer (ESO) is designed to estimate the disturbance from load offsetting. A kinematics controller is proposed to produce desired velocities for the differential drive mobile robot in outer loop. A dynamics controller is designed to track the desired velocities from kinematics controller in inner loop. Based on Lyapunov method, stability analyses are given for the nonlinear ESO, the kinematics controller and the dynamics controller. Simulations are carried out to illustrate effectiveness of the double closed-loop tracking control strategy.*
Keywords: Differential drive mobile robot, Load offsetting, Double closed-loop control, Nonlinear extended state observer, Trajectory tracking

1. **Introduction.** With the development of intelligent logistics, smart mobile robots are widely used in the field of warehouse logistics due to high automation and flexibility [1]. As one of intelligent mobile robots, differential drive mobile robots play an important role in the logistics field. Popular for its low cost, it has been more widely used in the logistics [2, 3]. Due to attractive prospects for development, the motion control schemes for the differential drive robots emerge endlessly [4, 5, 6]. In practical engineering applications, there are some internal disturbances and external uncertainties, which need to be considered in the design of trajectory tracking control strategy. Therefore, many control schemes have been designed to compensate these disturbances. An adaptive neural network control strategy is proposed for uncertain wheeled mobile robots with velocity and nonholonomic constraints [7]. A vision adaptive controller is proposed for mobile robots with uncertain conditions in complex environments [8]. In addition, a sliding mode control method combining ESO is designed to solve external interference and parameter uncertainty of wheeled mobile robots [9]. Comparing the above methods, the method using ESO is a better way to eliminate disturbances in a nonlinear and disturbed system [10].

It is well known that many control strategies with ESO have been developed and widely used in engineering practice [11, 12]. A friction compensation model predictive control method with ESO is proposed for the dynamics model of omnidirectional mobile robots with unknown friction [13]. In intelligent logistics, load offsetting is obviously an inevitable problem which causes centroid offsetting for the differential drive mobile robots [14]. Therefore, it is necessary to design a control strategy to ensure the robustness for differential drive mobile robots with load offsetting. Inspired by the above research work,

a nonlinear ESO is used to estimate the disturbance from load offsetting in differential drive mobile robots.

A double closed-loop tracking control strategy is designed for a differential drive mobile robot with load offsetting in this paper. A nonlinear ESO is given to estimate the disturbance caused by load offsetting. In the outer loop, a kinematics controller is designed for outputting desired velocities for the differential drive mobile robots. In the inner loop, a dynamics controller is designed to track the desired velocities from the outer loop. Based on Lyapunov method, the stability analyses are given for the nonlinear ESO, the kinematics controller and the dynamics controller. Effectiveness of the proposed double closed-loop tracking control strategy is shown by simulations results.

This paper is organized as follows. Section 2 presents the model of the differential drive mobile robot with load offsetting. Section 3 describes the design of the double closed-loop tracking control strategy. Simulations results of the proposed control strategy are given in Section 4, followed by the conclusion in Section 5.

Notations: In this paper, symbol $\text{sgn}(\cdot)$ is a standard sign function. $\text{diag}\{X_1, X_2\}$ is a diagonal matrix with diagonal elements being X_1, X_2. $\text{fal}(\cdot)$ is a nonlinear function given by

$$\text{fal}(\epsilon(t), \sigma, \delta) = \begin{cases} \epsilon(t)/\delta^{1-\sigma}, & |\epsilon(t)| \leq \delta \\ |\epsilon(t)|^{\sigma}\text{sgn}(\epsilon(t)), & |\epsilon(t)| > \delta \end{cases}$$

where σ and δ are satisfied with $0 < \sigma < 1$, $\delta \geq 0$, and $\epsilon(t)$ is a variable. Function $\text{fal}(\epsilon(t), \sigma, \delta)$ is expressed as $\text{fal}(\epsilon(t))$ for the sake of simplicity.

2. **Model of the Differential Drive Mobile Robot.** The schematic diagram of the differential drive mobile robot with load offsetting is shown in Figure 1. The motion of the differential drive mobile robot satisfies a condition of nonholonomic constraint. A constraint equation is written as $A(q(t))\dot{q}(t) = 0$, where $q(t) = [x(t), y(t), \theta(t)]^T$ is the global coordinate vector, and $A(q(t)) = [\sin(\theta(t)), -\cos(\theta(t)), d\cos\alpha]$ is a kinematics constraint vector.
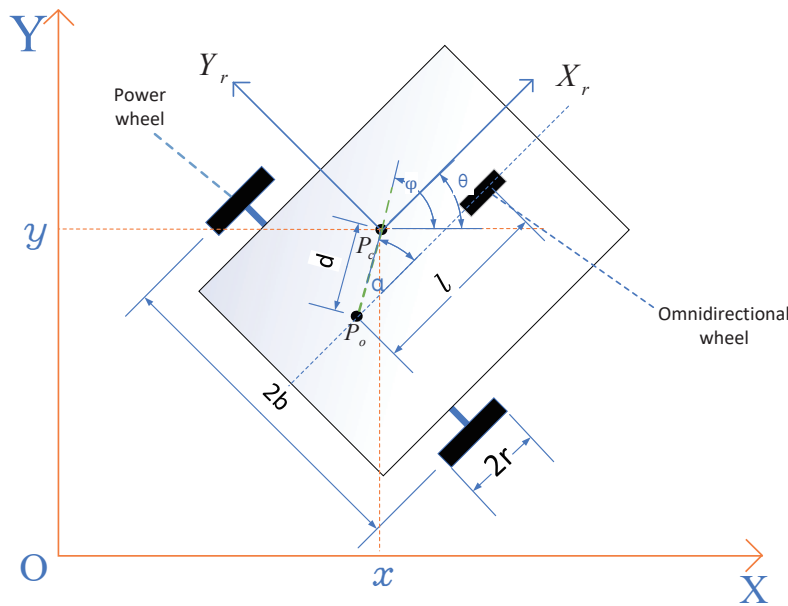

FIGURE 1. Coordinate representation of the mobile robot with load offsetting

The kinematics model of the differential drive mobile robot is obtained as:

$$\dot{q}(t) = S(q(t))V(t) \tag{1}$$

where $V(t) = [v(t), w(t)]^T$ is the velocity vector of the differential drive mobile robot, $v(t)$ is the linear velocity and $w(t)$ is the angular velocity, the Jacobian matrix $S(q(t))$ is written as

$$S(q(t)) = \begin{bmatrix} \cos(\theta(t)) & -d\sin(\varphi(t)) \\ \sin(\theta(t)) & d\cos(\varphi(t)) \\ 0 & 1 \end{bmatrix}$$

For the differential drive mobile robot, the left and right power wheels are driven by DC motors through the gearboxes. A simplified diagram of the motor drive system is shown in Figure 2.
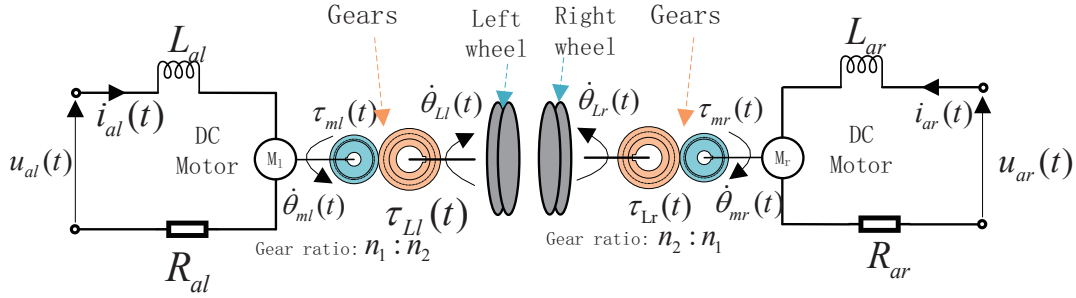

FIGURE 2. Power wheels drive system

The relationship between the driving torques of the two power wheels and the voltages of the DC motors is written as follows:

$$\tau_m(t) = M_1 u_c(t) - M_2 B_0 V(t) = M_1 u_c(t) - \frac{M_2}{r} \begin{bmatrix} 1 & b \\ 1 & -b \end{bmatrix} V(t) \tag{2}$$

where $\tau_m(t) = [\tau_{mr}(t), \tau_{ml}(t)]^T$, $u_c(t) = [u_{ar}(t), u_{al}(t)]^T$ are the driving torque vector and the input voltages of the DC motors, respectively, $M_1 = n_2 K_a / n_1 R_a$, $M_2 = n_2 M_1 K_e / n_1$, K_a is a torque constant, K_e is a back EMF constant, n_1 and n_2 are the numbers of motor gear teeth and power wheel gear teeth, respectively, and $R_a = R_{al} = R_{ar}$ is the resistance value in the circuit.

Based on Euler-Lagrange equation, the dynamics model of the differential drive mobile robot is obtained as follows [15]:

$$M(q(t))\ddot{q}(t) + C(q(t), \dot{q}(t))\dot{q}(t)$$
$$= B(q(t))\tau(t) - G(q(t)) - F(\dot{q}(t)) - \tau_d(t) - \lambda_1 A^T(q(t)) \tag{3}$$

where λ_1 is a constraint multiplier, $G(q(t)) = 0$ is the gravity vector, and $\tau_d(t)$ represents the unknown interference, which is not considered in this paper. $F(\dot{q}(t))$ is the friction between the differential drive mobile robot and the ground, and the positive definite symmetric inertia matrix $M(q(t))$, the centripetal and Coriolis matrix $C(q(t), \dot{q}(t))$ and the input transformation matrix $B(q(t))$ are obtained as follows:

$$M(q(t)) = \begin{bmatrix} m & 0 & md\sin(\varphi(t)) \\ * & m & -md\cos(\varphi(t)) \\ * & * & J + md^2 \end{bmatrix}, \quad B(q(t)) = \frac{1}{r} \begin{bmatrix} \cos(\theta(t)) & \cos(\theta(t)) \\ \sin(\theta(t)) & \sin(\theta(t)) \\ b & -b \end{bmatrix}$$

$$C(q(t), \dot{q}(t)) = \begin{bmatrix} 0 & 0 & md\dot{\varphi}(t)\cos(\varphi(t)) \\ 0 & 0 & md\dot{\varphi}(t)\sin(\varphi(t)) \\ 0 & 0 & 0 \end{bmatrix}$$

where m_1, m_w and m_l are the mass of the differential drive mobile robot, a power wheel and the load, respectively, $m = m_1 + m_l + 2m_w$ and $J = 2m_w b^2 + (m_1 + m_l)d^2$, μ is the rolling friction factor and g is the acceleration of gravity, then $F(\dot{q}(t))$ is given as

$$F(\dot{q}(t)) = B(q(t))r \begin{bmatrix} f_r \\ f_l \end{bmatrix} = B(q(t))r \begin{bmatrix} \mu(m_1 + m_l)g(l - d\cos\alpha)(b - d\sin\alpha)/2bl + \mu m_w g \\ \mu(m_1 + m_l)g(l - d\cos\alpha)(b + d\sin\alpha)/2bl + \mu m_w g \end{bmatrix}$$

Substituting Equations (1) and (2) into Equation (3), and multiplying left with $S^T(q(t))$ on both sides, Equation (3) is written as

$$\bar{M}_c \dot{V}(t) + \bar{M}_l \dot{V}(t) + \bar{C}V(t) + \bar{f}(t) = \bar{B}_0 u(t) \tag{4}$$

where

$$\bar{C} = \frac{2M_2}{r^2} \begin{bmatrix} 1 & 0 \\ -d\sin\alpha & b^2 \end{bmatrix}$$

and $\bar{f}(t) = S^T(q(t))F(\dot{q}(t))$, $\bar{M}_c = \text{diag}\{(m_1 + 2m_w)\cos\alpha, 2m_w b^2 + I_1\}$, $\bar{M}_l = \text{diag}\{m_l \cos\alpha, I_2\}$, $\bar{B}_0 = \frac{M_1}{r}\text{diag}\{1, b\}$, I_1 and I_2 are the moments of inertia to the point P_o of the robot and the load, respectively, $u(t) = [u_1(t), u_2(t)]^T$ with $u_1(t) = u_{ar}(t) + u_{al}(t)$ and $u_2(t) = u_{ar}(t) - u_{al}(t)$. Letting $x_1(t) = V(t) = [x_{11}(t), x_{12}(t)]^T = [v(t), w(t)]^T$ and shifting the term of Equation (4), one has that

$$\dot{x}_{1i}(t) = f_{0i}(t) + b_{0i}u_i(t) \tag{5}$$

where $f_0(t) = -\bar{M}_c^{-1}\left[\bar{M}_l \dot{V}(t) + \bar{C}V(t) + \bar{f}(t)\right] = [f_{01}(t), f_{02}(t)]^T$ and $b_0 = \bar{M}_c^{-1}\bar{B}_0 = \text{diag}\{b_{01}, b_{02}\}$.

Assumption 2.1. *For the disturbance $f_0(t)$ in Equation (5), assume it is continuously differentiable and bounded. That is, there is a constant N_0 satisfying $|f_0(t)| \leq N_0$.*

Remark 2.1. *Due to the fact that the angular velocity dynamic model is similar to the linear velocity one, only the linear velocity dynamics model is considered for the sake of simplicity. Therefore, the linear velocity dynamics model is considered in stability analyses of the nonlinear ESO and the dynamics controller.*

3. **Main Results.** In this section, a double closed-loop tracking control strategy is designed to achieve trajectory tracking for a differential drive mobile robot with load offsetting. The structure of the double closed-loop tracking control strategy is shown in Figure 3. A nonlinear ESO is designed to estimate the disturbance from load offsetting. A kinematics controller of the outer loop is given to produce the desired velocities for the differential drive mobile robot. A dynamics controller of the inner loop is proposed to track the desired velocities. T_e is a transformation matrix between global coordinate and local coordinate.
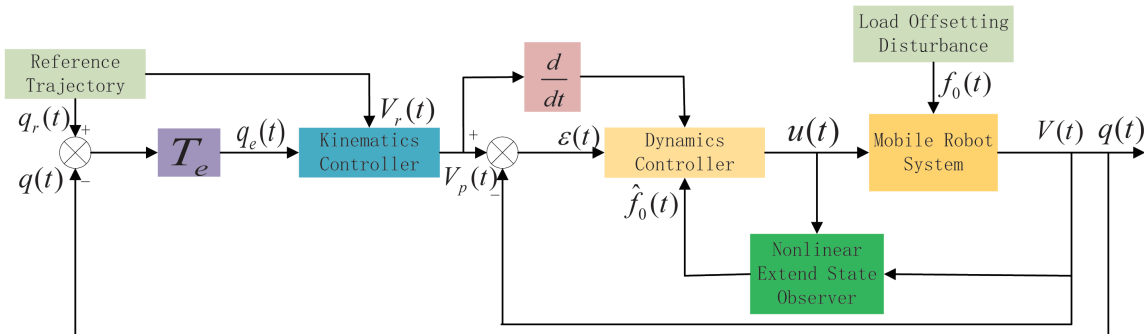

FIGURE 3. The structure of the double closed-loop tracking control strategy

3.1. **Nonlinear extended state observer.** For the differential drive mobile robot, the control performance is affected due to the disturbance $f_0(t)$ in the inner loop. Therefore, a nonlinear ESO is designed to estimate the disturbance. $f_0(t)$ is extended to a new state $x_2(t)$, which is shown that $x_2(t) = [x_{21}(t), x_{22}(t)]^T = [f_{01}(t), f_{02}(t)]^T$. Based on Assumption 2.1, the dynamics system is described as

$$\dot{x}_{1i}(t) = x_{2i}(t) + b_{01}u_i(t) \tag{6}$$
$$\dot{x}_{2i}(t) = \omega_i(t) \tag{7}$$

where $\omega(t) = [\omega_1(t), \omega_2(t)]^T$, in which $\omega_i(t)$ with $i = 1, 2$ is a bounded continuous function. The nonlinear ESO for the dynamics system (6) and (7) is designed as follows

$$\dot{\hat{x}}_{1i}(t) = \hat{x}_{2i}(t) - \beta_{1i}e_{1i}(t) + b_{0i}u_i(t) \tag{8}$$
$$\dot{\hat{x}}_{2i}(t) = -\beta_{2i}\text{fal}(e_{1i}(t), \sigma, \delta) \tag{9}$$

where $\hat{x}_{1i}(t)$ and $\hat{x}_{2i}(t)$ are the estimation values of $x_{1i}(t)$ and $x_{2i}(t)$, respectively, $e_{1i}(t) = \hat{x}_{1i}(t) - x_{1i}(t)$ with $i = 1, 2$ is the estimation error, β_{1i} and β_{2i} with $i = 1, 2$ are appropriate positive constants.

Considering the dynamics system (6) and (7) and the nonlinear ESO (8) and (9), an estimation error system is given as

$$\dot{e}_{1i}(t) = e_{2i}(t) - \beta_{1i}e_{1i}(t) \tag{10}$$
$$\dot{e}_{2i}(t) = -\omega_i(t) - \beta_{2i}\text{fal}(e_{1i}(t), \sigma, \delta) \tag{11}$$

where $e_{2i}(t) = \hat{x}_{2i}(t) - x_{2i}(t)$ with $i = 1, 2$ is the estimation error of the disturbance. Stability analysis of the nonlinear ESO (8) and (9) is given in the following theorem.

Theorem 3.1. *The estimation errors $e_{1i}(t)$ and $e_{2i}(t)$ are bounded by giving appropriate positive parameters β_{1i} and β_{2i} with $i = 1, 2$. That is, the estimation error system (10) and (11) is asymptotically stable by the nonlinear ESO (8) and (9).*

Proof: A Lyapunov function is given by

$$V_1(t) = \lambda_1|e_{11}(t)|^{\frac{3}{2}} - \lambda_2 e_{11}(t)e_{21}(t) + \lambda_3 e_{21}(t)^2 \tag{12}$$

where λ_1, λ_2, and λ_3 are constants which are satisfied with $\lambda_1 > 0$, $\lambda_2 > 0$, $\lambda_3 > 0$, $\lambda_2{}^2 - 4\lambda_1\lambda_3 < 0$. Therefore, it is obtained that $V_1(t)$ is positive according to (12). The derivative of Equation (12) is given as follows

$$\begin{aligned}\dot{V}_1(t) &= \frac{\partial V_1(t)}{\partial e_{11}(t)}\dot{e}_{11}(t) + \frac{\partial V_1(t)}{\partial e_{21}(t)}\dot{e}_{21}(t) \\&= -A|e_{11}(t)|^{2\left(\frac{3}{4}\right)} + B|e_{11}(t)|^{\frac{3}{4}}\text{sgn}(e_{11}(t))e_{21}(t) - Ce_{21}(t)^2 \\&\quad + \omega_1(t)(\lambda_2 e_{11}(t) - 2\lambda_3 e_{21}(t))\end{aligned} \tag{13}$$

where $A = \left(\frac{3}{2}\lambda_1\beta_{11} - \lambda_2\beta_{21}\right)$, $B = \left[\frac{3}{2}\lambda_1 - 2\lambda_3\beta_{21} + \lambda_2\beta_{11}|e_{11}(t)|^{\frac{1}{2}}\right]|e_{11}(t)|^{-\frac{1}{4}}$ and $C = \lambda_2$. The quadratic part of Equation (13) is negative if $A > 0$, $B > 0$, $C > 0$ and $B^2 - 4AC < 0$ hold. That is, $3\lambda_1/\lambda_2 > 2\beta_{21}/\beta_{11}$, $3\lambda_1 > 4\lambda_3\beta_{21}$, $\lambda_2 > 0$, and

$$\frac{3}{2}\lambda_1 - 2\lambda_3\beta_{21} + \lambda_2\beta_{11}|e_{11}(t)|^{\frac{1}{2}} < 2\sqrt{\lambda_2\left(\frac{3}{2}\lambda_1\beta_{11} - \lambda_2\beta_{21}\right)}|e_{11}(t)|^{\frac{1}{4}}$$

Letting $a = \lambda_2\beta_{11}$, $b = \sqrt{\lambda_2\left(\frac{3}{2}\lambda_1\beta_{11} - \lambda_2\beta_{21}\right)}$, $c = \frac{3}{2}\lambda_2 - 2\lambda_3\beta_{21}$, and $x(t) = |e_{11}(t)|^{\frac{1}{4}}$, it is obtained that $c + ax^2(t) < 2bx(t)$. For this inequality to make sense $x(t)$ has to satisfy $b^2 - ac > 0$, it holds between two roots of the quadratic equation $ax^2(t) - 2bx(t) + c = 0$. Select a large $\delta = b^2 - ac > 0$ to ensure that the interval between the two roots of

Equation (13) is large, and pick a suitable λ_3 to make $2\lambda_3\beta_{11} - \lambda_2 > 0$ large. Therefore, the coefficients of the Lyapunov function (12) satisfy the following inequalities

$$\lambda_2 > 0, \ 3\frac{\lambda_1}{\lambda_2} > 2\frac{\beta_{21}}{\beta_{11}}, \ 3\lambda_1 > 4\lambda_3\beta_{21}$$

It guarantees that the Lyapunov function (12) satisfies the positive definite condition. In this case, for any $e_{21}(t)$ and for a large range of $e_{11}(t)$, $\dot{V}_1(t)$ is negative definite. However, when the parameters are selected in the above way, the negative definite condition is not satisfied on the intersection line of parabola $Z_1(t) = -A|e_{11}(t)|^{2\left(\frac{3}{4}\right)} + B|e_{11}(t)|^{\frac{3}{4}}\mathrm{sgn}(e_{11}(t))e_{21}(t) - Ce_{21}(t)^2$ and plane $Z_2(t) = -\lambda_2\omega_1(t)e_{11}(t) - 2\lambda_3\omega_1(t)e_{21}(t)$. The $e_{11}(t)$ and the $(\lambda_2\omega_1(t)/A)^2$ on this intersection are the same order of magnitude. Then it can be deduced that $e_{11}(t)$ and $(\omega_1(t)/\beta_{21})^2$ are of the same order of magnitude. Therefore, adjusting parameters β_{21} makes error $e_{11}(t)$ bounded. That is, the estimation values $\hat{x}_{11}(t)$ and $\hat{x}_{21}(t)$ of the nonlinear ESO (8) and (9) is effective.

3.2. **Kinematics controller.** A kinematics controller is proposed to give the desired velocities for the differential drive mobile robot. $q_r(t) = [x_r(t), y_r(t), \theta_r(t)]^T$ represents the reference trajectory, and the tracking error between real differential drive mobile robot and reference differential drive mobile robot is given as $q_e(t) = T_e(q_r(t) - q(t)) = [e_x(t), e_y(t), e_\theta(t)]^T$, where

$$T_e = \begin{bmatrix} \cos\theta(t) & \sin\theta(t) & 0 \\ -\sin\theta(t) & \cos\theta(t) & 0 \\ 0 & 0 & 1 \end{bmatrix}$$

To facilitate the design of kinematics controller, letting $\tilde{e}_x(t) = e_x(t) + d(1 - \cos e_\theta(t))$, $\tilde{e}_y(t) = e_y(t) - d\sin e_\theta(t)$, the tracking error system is obtained as

$$\begin{cases} \dot{\tilde{e}}_x(t) = w(t)\tilde{e}_y(t) + v_r(t)\cos e_\theta(t) - v(t) \\ \dot{\tilde{e}}_y(t) = -w(t)\tilde{e}_x(t) + v_r(t)\sin e_\theta(t) \\ \dot{e}_\theta(t) = w_r(t) - w(t) \end{cases} \tag{14}$$

Based on back-stepping method and the tracking error system (14), a kinematics controller is designed as follows

$$V_p(t) = \begin{bmatrix} v_p(t) \\ w_p(t) \end{bmatrix} = \begin{bmatrix} k_1\tilde{e}_x(t) + v_r(t)\cos e_\theta(t) \\ w_r(t) + k_2v_r(t)\tilde{e}_y(t) + k_3v_r(t)\sin e_\theta(t) \end{bmatrix} \tag{15}$$

Theorem 3.2. *For the kinematics controller* (15), *the tracking error system* (14) *is asymptotically stable by selecting appropriate positive parameters* k_1, k_2 *and* k_3.

Proof: A Lyapunov function is given as

$$V_2(t) = \frac{1}{2}\left[\tilde{e}_x^2(t) + \tilde{e}_y^2(t)\right] + \frac{1}{k_2}[1 - \cos e_\theta(t)] \tag{16}$$

Based on the following tracking error system, one has that

$$\begin{aligned} \dot{V}_2(t) = & \left[(w_r(t) + v_r(t)(k_2\tilde{e}_y(t) + k_3\sin e_\theta(t)))\tilde{e}_y(t) - k_1\tilde{e}_x(t)\right]\tilde{e}_x(t) \\ & + \left[-(w_r(t) + v_r(t)(k_2\tilde{e}_y(t) + k_3\sin e_\theta(t)))\tilde{e}_x(t) + v_r(t)\sin e_\theta(t)\right]\tilde{e}_y(t) \\ & + \frac{1}{k_2}\left[-v_r(t)(k_2\tilde{e}_y(t) + k_3\sin e_\theta(t))\right]\sin e_\theta(t) \\ = & -k_1\tilde{e}_x(t)^2 - \frac{k_3}{k_2}v_r(t)\sin^2 e_\theta(t) \leq 0 \end{aligned}$$

Therefore, the tracking error system (14) is asymptotically stable with appropriate positive parameters k_1, k_2 and k_3.

3.3. **Dynamics controller.** In the inner loop of the double closed-loop control strategy, a dynamics controller is designed to track the desired velocities from the outer loop. Let $x_p(t) = V_p(t) = [x_{p1}, x_{p2}] = [v_p(t), w_p(t)]^T$, the tracking error of the inner loop is $\varepsilon_i(t) = x_{pi}(t) - x_{1i}(t)$ with $i = 1, 2$. Considering Equation (6), the derivative of $\varepsilon_i(t)$ is shown as $\dot{\varepsilon}_i(t) = \dot{x}_{pi}(t) - x_{2i}(t) - b_{0i}u_i(t)$ with $i = 1, 2$. The sliding mode surface is selected as $s_i(t) = \varepsilon_i(t) + h_{1i}\int_0^t \text{fal}(\varepsilon_i(t))dt$, where h_{1i} with $i = 1, 2$ is a positive constant. The derivative of the sliding mode surface $s_i(t)$ is shown as $\dot{s}_i(t) = \dot{x}_{pi}(t) - x_{2i}(t) - b_{0i}u_i(t) + h_{1i}\text{fal}(\varepsilon_i(t))$ with $i = 1, 2$. A reaching law is designed as $\dot{s}_i(t) = -h_{2i}s_i(t) - h_{3i}\text{sgn}(s_i(t))$ with $i = 1, 2$, and a dynamics controller is obtained as

$$u_i(t) = \frac{1}{b_{0i}}\left[\dot{x}_{pi}(t) - \hat{x}_{2i}(t) + h_{1i}\text{fal}(\varepsilon_i(t)) + h_{2i}s_i(t) + h_{3i}\text{sgn}(s_i(t))\right] \tag{17}$$

where h_{2i} and h_{3i} with $i = 1, 2$ are positive constants. Effectiveness of the control law (17) is shown in the following theorem.

Theorem 3.3. *The tracking error of the inner loop $\varepsilon_i(t)$ with $i = 1, 2$ is convergent by selecting suitable positive parameters h_{1i}, h_{2i} and h_{3i} with $i = 1, 2$.*

Proof: A Lyapunov function is chosen as $V_3(t) = \frac{1}{2}s_1^2(t)$, and one has that

$$\begin{aligned}
\dot{V}_3(t) &= s_1(t)\dot{s}_1(t) \\
&= s_1(t)\left(e_{21}(t) - h_{21}s_1(t) - h_{31}\text{sgn}(s_1(t))\right) \\
&\leq e_{21}(t)|s_1(t)| - h_{21}s_1^2(t) - h_{31}|s_1(t)|
\end{aligned} \tag{18}$$

where $e_{21}(t)$ is bounded according to the nonlinear ESO design. Therefore, there exists a positive constant N_2 such that $e_{21}(t) \leq N_2$. Inequality (18) will be rewritten as

$$\dot{V}_3(t) \leq -(h_{31} - N_2)|s_1(t)| - h_{21}s_1^2(t)$$

The inequality $\dot{V}_3(t) < 0$ holds by selecting the appropriate parameter h_{31}. Therefore, the tracking error system is asymptotically stable, and the dynamics controller (17) designed in this paper is effective.

4. **Simulations Results.** In this section, simulations are carried out to verify effectiveness of the double closed-loop control strategy for the differential drive mobile robot with load offsetting. In the simulations, the physical parameters of the differential drive mobile robot are set as $m_1 = 3.6$ kg, $m_w = 0.5$ kg, $r = 0.12$ m, $b = 0.166$ m, $l = 0.4$ m, $g = 9.8$ m/s^2, $\mu = 0.015$, $M_1 = 0.64$ and $M_2 = 0.96$. The distance d, the angle α and the weight m_l are the load offset parameters of the differential drive mobile robot. The sampling period is $T = 0.01$ s in the simulations. The initial values and velocities of reference trajectory and real trajectory are set as $(x_r(0), y_r(0), \theta_r(0)) = (3.0 \text{ m}, 1.0 \text{ m}, 0 \text{ rad})$, $v_r = 0.4$ m/s, $w_r = 0.6$ rad/s, $(x(0), y(0), \theta(0)) = (3.0 \text{ m}, 0.8 \text{ m}, 15 \text{ rad})$, $v(0) = 0.3$ m/s and $w(0) = 0.5$ rad/s. The parameters used in the nonlinear ESO (8) and (9), the kinematics controller (15) and the dynamics controller (17) are listed in Table 1. In the simulations of the circular trajectory tracking, two different tracking trajectories are obtained by changing the load offset parameters of the differential drive mobile robot, and the simulations results are shown in Figure 4(a).

It is shown that the differential drive mobile robot effectively tracks the reference trajectory. For the different load offset parameters, the differential drive mobile robot keeps

TABLE 1. Controller parameters in the simulations

Nonlinear ESO	$\beta_{1i} = 300$	$\beta_{2i} = 1000$	$\sigma = 0.25$	$\delta = 0.01$	
Kinematic controller	$k_1 = 1.5$	$k_2 = 5$	$k_3 = 5$		
Dynamics controller	$h_{1i} = 25$	$h_{2i} = 25$	$h_{3i} = 0.1$	$\sigma_i = 0.25$	$\delta_i = 0.05$
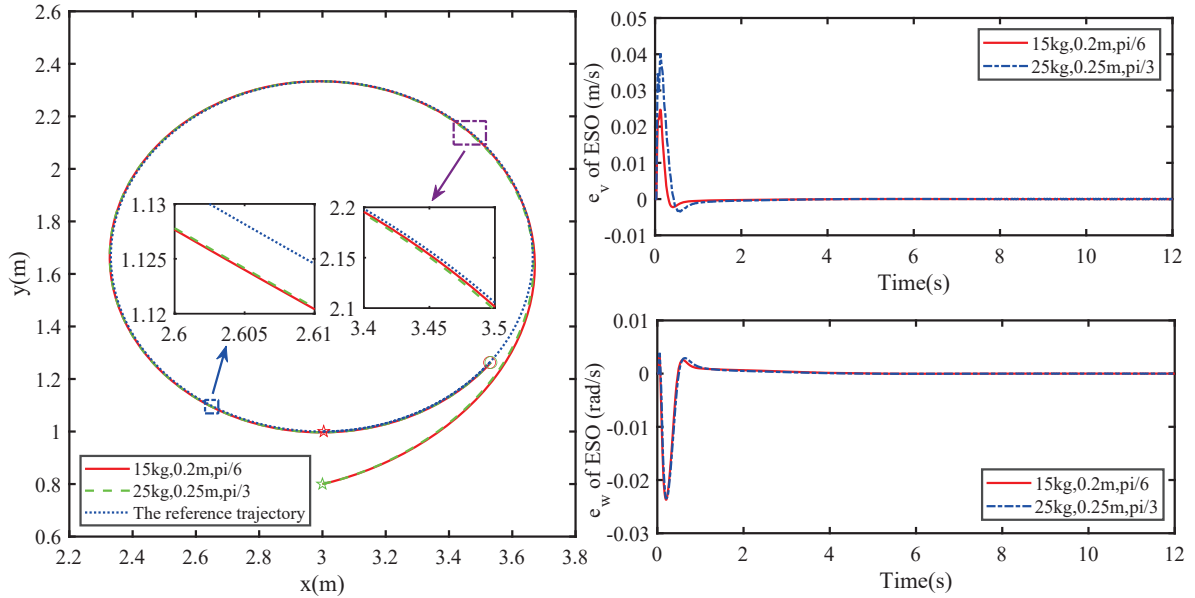
(a) Circular trajectory tracking results
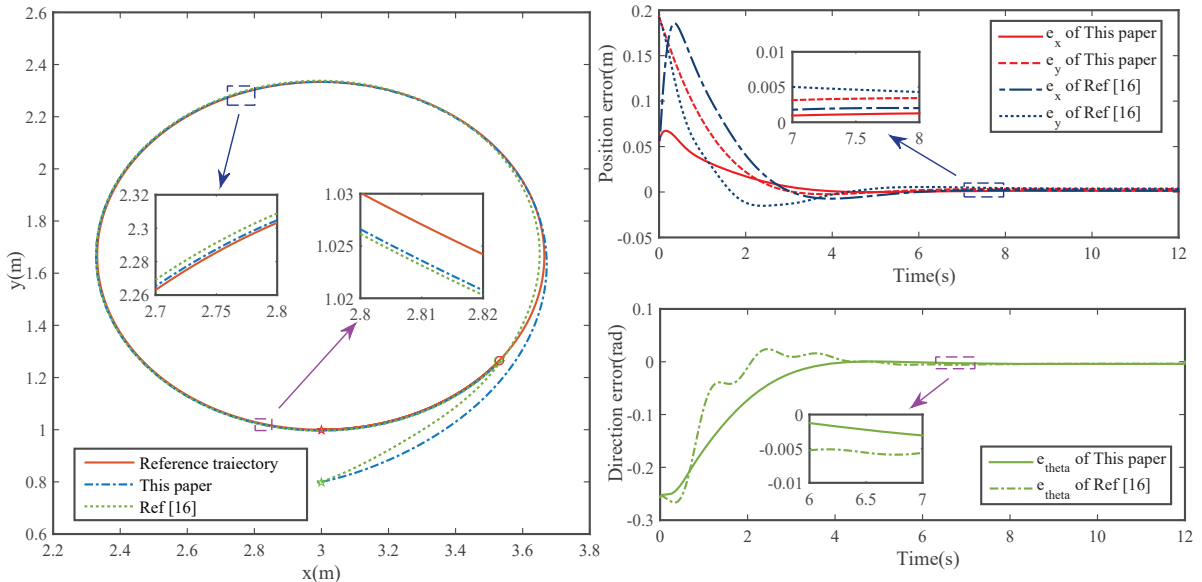
(b) Comparison results of the tracking trajectory

FIGURE 4. Simulations results

up with the reference trajectory. To show superiority of the double closed-loop tracking control strategy, a simulation has been carried out for the method of [16] and the double closed-loop tracking control strategy. The comparison results of the tracking trajectory are given in Figure 4(b). It is shown that the tracking effect of this paper is better than that of [16]. Therefore, it illustrates the effectiveness and superiority of the double closed-loop control strategy proposed in this paper.

5. **Conclusion.** In this paper, a double closed-loop trajectory tracking strategy is designed for a differential drive mobile robot with load offsetting. A nonlinear ESO is used to estimate the disturbance from load offsetting. A kinematics controller of the outer loop is used to deal with the nonholonomic constraints of the differential drive mobile robot. In the inner loop of the double closed-loop trajectory tracking strategy, a dynamics controller is designed to track the desired velocities from the outer loop. Based on Lyapunov method, stability analyses are given for the nonlinear ESO, the kinematics controller and

the dynamics controller. Simulations results illustrate effectiveness of the double closed-loop tracking control strategy. In the further work, it is of great significance to promote the development of differential drive mobile robot prototypes.

REFERENCES

[1] C. Lee, B. Lin, K. Ng, Y. Lv and W. C. Tai, Smart robotic mobile fulfillment system with dynamic conflict-free strategies considering cyber-physical integration, *Advanced Engineering Informatics*, vol.42, 100998, 2019.

[2] R. Hou, L. Cui, X. Bu and J. Yang, Distributed formation control for multiple non-holonomic wheeled mobile robots with velocity constraint by using improved data-driven iterative learning, *Applied Mathematics and Computation*, vol.395, 2021.

[3] Y. Wu, Y. Wang and H. Fang, Full-state constrained neural control and learning for the nonholonomic wheeled mobile robot with unknown dynamics, *ISA Transactions*, DOI: 10.1016/j.isatra.2021.06.012, 2021.

[4] F. Sun, H. Li, W. Zhu and J. Kurths, Fixed-time formation tracking for multiple nonholonomic wheeled mobile robots based on distributed observer, *Nonlinear Dynamics*, vol.106, no.4, pp.3331-3349, 2021.

[5] J. Wu, D. Fu, Y. Liu and B. Sun, Trajectory following control for autonomous vehicles using the feed-forward controller and the improved trajectory following model, *International Journal of Innovative Computing, Information and Control*, vol.17, no.6, pp.2019-2032, 2021.

[6] M. Ou, H. Sun, Z. Zhang and S. Gu, Fixed-time trajectory tracking control for nonholonomic mobile robot based on visual servoing, *Nonlinear Dynamics*, vol.108, no.1, pp.251-263, 2022.

[7] Z. Chen, Y. Liu, W. He and H. Qiao, Adaptive-neural-network-based trajectory tracking control for a nonholonomic wheeled mobile robot with velocity constraints, *IEEE Transactions on Industrial Electronics*, vol.68, no.6, pp.5057-5067, DOI: 10.1109/TIE.2020.2989711, 2021.

[8] F. Wang, Y. Qin, F. Guo, B. Ren and J. Yeow, Adaptive visually servoed tracking control for wheeled mobile robot with uncertain model parameters in complex environment, *Complexity*, vol.2020, no.3, pp.1-13, 2020.

[9] K. Liu, H. Ji and Y. Zhang, Extended state observer based adaptive sliding mode tracking control of wheeled mobile robot with input saturation and uncertainties, *Proc. of the Institution of Mechanical Engineers, Part C. Journal of Mechanical Engineering Science*, vol.233, no.15, 2019.

[10] H. S. Kang, Y. T. Kim, C. H. Hyun and M. Park, Generalized extended state observer approach to robust tracking control for wheeled mobile robot with skidding and slipping, *International Journal of Advanced Robotic Systems*, vol.10, no.3, pp.463-474, 2013.

[11] S. Li, J. Yang, W. H. Chen and X. Chen, Generalized extended state observer based control for systems with mismatched uncertainties, *IEEE Transactions on Industrial Electronics*, vol.59, no.12, pp.4792-4802, 2012.

[12] B. Xu, S. Ji, C. Zhang, C. Chen and X. Wu, Linear-extended-state-observer-based prescribed performance control for trajectory tracking of a robotic manipulator, *Industrial Robot*, vol.48, pp.544-555, 2021.

[13] C. Ren, R. Liu, S. Ma, C. Hu and L. Cao, ESO based model predictive control of an omnidirectional mobile robot with friction compensation, *China Control Conference*, vol.37, pp.508-513, 2018.

[14] Y. Farid, V. J. Majd and A. Ehsani-Seresht, Fractional-order active fault-tolerant force-position controller design for the legged robots using saturated actuator with unknown bias and gain degradation, *Mechanical Systems & Signal Processing*, DOI: 10.1016/j.ymssp.2017.11.010, 2018.

[15] K. Wu, W. Li, C. Liu and G. Li, Dynamics control of a two-wheel drive mobile robot, *Journal of Aerospace*, vol.27, no.2, 2006.

[16] H. Yang, Y. Xia, C. Hua and X. Fan, Robust tracking control for wheeled mobile robot based on extended state observer, *Advanced Robotics: The International Journal of the Robotics Society of Japan*, vol.30, no.2, pp.68-78, 2016.